MOLECULAR AND CELLULAR BIOLOGY, Feb. 2006, p. 898–911 Vol. 26, No. 3
0270-7306/06/$08.00+0 doi:10.1128/MCB.26.3.898–911.2006

Glycogen Synthase Kinase 3 and h-prune Regulate Cell Migration by Modulating Focal Adhesions†

Tsuyoshi Kobayashi,[1,2] Shin-ichiro Hino,[1] Naohide Oue,[3] Toshimasa Asahara,[2] Massimo Zollo,[4] Wataru Yasui,[3] and Akira Kikuchi[1]*

Departments of Biochemistry,[1] Surgery,[2] and Molecular Pathology,[3] Graduate School of Biomedical Sciences, Hiroshima University, Hiroshima, Japan, and CEINGE, Biotecnologie Avanzate s.c.ar.l., Napoli, Italy[4]

Received 25 July 2005/Returned for modification 2 September 2005/Accepted 4 November 2005

h-prune, which has been suggested to be involved in cell migration, was identified as a glycogen synthase kinase 3 (GSK-3)-binding protein. Treatment of cultured cells with GSK-3 inhibitors or small interfering RNA (siRNA) for GSK-3 and h-prune inhibited their motility. The kinase activity of GSK-3 was required for the interaction of GSK-3 with h-prune. h-prune was localized to focal adhesions, and the siRNA for GSK-3 or h-prune delayed the disassembly of paxillin. The tyrosine phosphorylation of focal adhesion kinase (FAK) and the activation of Rac were suppressed in GSK-3 or h-prune knocked-down cells. GSK-3 inhibitors suppressed the disassembly of paxillin and the activation of FAK and Rac. Furthermore, h-prune was highly expressed in colorectal and pancreatic cancers, and the positivity of the h-prune expression was correlated with tumor invasion. These results suggest that GSK-3 and h-prune cooperatively regulate the disassembly of focal adhesions to promote cell migration and that h-prune is useful as a marker for tumor aggressiveness.

The serine/threonine kinase glycogen synthase kinase 3 (GSK-3) was first described for a metabolic pathway for glycogen synthase regulation that is sensitive to insulin-mediated inhibition (35). GSK-3 has subsequently been shown to regulate several physiological responses, including protein synthesis, gene expression, subcellular localization of proteins, and protein degradation, in mammalian cells by phosphorylating many substrates (5, 9, 16). There are two members of GSK-3α and GSK-3β in mammals (49). GSK-3 is highly conserved through evolution and plays a fundamental role in cellular responses. For example, there are four genes, *MCK1*, *MDS1*/*RIM11*, *MRK1*, and *YOL128c*, which encode homologs of mammalian GSK-3 in *Saccharomyces cerevisiae*. Mck1 stabilizes Rog1 (1) and stimulates gene expression by Msn2 in yeasts (19).

To understand the molecular mechanism by which GSK-3 recognizes specific target substrates, we have tried to isolate proteins that bind to GSK-3. So far, we have identified Axin, Axil, and AKAP220 as GSK-3β-binding proteins (21, 43, 52). Axin binds to not only GSK-3 but also β-catenin, APC, and Dvl, all of which are important components in the Wnt signaling pathway (25, 48). In the Axin complex, GSK-3 phosphorylates β-catenin, APC, and Axin efficiently (21, 27) and thereby induces ubiquitination of β-catenin, leading to its degradation. Axil has characteristics similar to those of Axin (52). AKAP220 binds to not only GSK-3 but also cyclic AMP (cAMP)-dependent protein kinase and protein phosphatase 1 (43). The phosphorylation and dephosphorylation of GSK-3 occur efficiently in the AKAP220 complex. Therefore, GSK-3 may exhibit different functions and regulation depending on its binding partners.

Evidence that GSK-3 regulates cellular architecture in neuronal cells has been accumulated (5, 24). Two microtubule-associating proteins, Tau and MAP1B, are phosphorylated by GSK-3, which regulates their binding to microtubules, thereby modulating microtubule dynamics. An inactive pool of GSK-3 has been found to be localized at the leading edge of the cells alongside F-actin, and semapholin 3A and lysophosphatidic acid activate GSK-3, causing growth cone collapse and neurite retraction (10). GSK-3 mediates Par6-PKCζ-dependent promotion of polarization and cell protrusion in astrocytes (11). Furthermore, GSK-3 phosphorylates CRMP2 to specify the fate of axons and dendrites (54). GSK-3 has also been shown to be involved in signaling activated by cell adhesion in nonneuronal cells (23, 37). The formation of extending lamellipodia in migrating keratinocytes is blocked by GSK-3 inhibitors (29). The initiation and stimulation of sperm motility are accompanied by the inactivation of GSK-3 (41). Although these results suggest that GSK-3 is involved in the dynamics of actin filaments and microtubules, how the GSK-3 activity is linked to molecules involved in cell migration is not clearly understood.

The human homolog of *Drosophila* prune protein (h-prune) belongs to the DHH superfamily of phosphodiesterases (PDE), which have cytoplasmic cyclic nucleotide phosphodiesterase activity (8). Overexpression of h-prune in cultured cells is involved in promoting cellular motility, and inhibition of PDE activity by a PDE inhibitor suppresses h-prune-induced motility (8). Consistent with these observations, overexpression of h-prune in breast cancer is correlated with cancer progression and aggressiveness (55). However, the molecular mechanism by which h-prune regulates cell motility remains to be defined.

To understand the molecular mechanism by which GSK-3 regulates cell migration, we screened new GSK-3-binding proteins. Here, we identified h-prune as a GSK-3-binding protein.

* Corresponding author. Mailing address: Department of Biochemistry, Graduate School of Biomedical Sciences, Hiroshima University, 1-2-3 Kasumi, Minami-ku, Hiroshima 734-8551, Japan. Phone: 81-82-257-5130. Fax: 81-82-257-5134. E-mail: akikuchi@hiroshima-u.ac.jp.

† Supplemental material for this article may be found at http://mcb.asm.org/.

Knockdown of GSK-3 and h-prune by small interfering RNA (siRNA) suppressed cell migration. h-prune formed a complex with paxillin and vinculin at focal adhesions. Loss of activity of GSK-3 or knockdown of GSK-3 and h-prune inhibited the disassembly of paxillin, the tyrosine phosphorylation of focal adhesion kinase (FAK), and the activation of Rac. These results indicate that GSK-3 and h-prune cooperatively regulate the disassembly of focal adhesions to regulate cell migration.

MATERIALS AND METHODS

Materials and chemicals. HeLa S3 and C57MG cells were provided by K. Matsumoto (Nagoya University, Nagoya, Japan) and S. Takada (National Institutes of Natural Sciences, Okazaki, Japan), respectively. Human GSK-3β cDNA was provided by J. R. Woodgett (Ontario Cancer Institute, Toronto, Canada). Recombinant baculoviruses expressing glutathione *S*-transferase (GST)-fused h-prune wild type (WT) were generated by Y. Matsuura (Osaka University, Suita, Japan). Paxillin cDNA and pGEX-αPAK-CRIB were provided by H. Sabe (Osaka Bioscience Institute, Osaka, Japan) and K. Kaibuchi (Nagoya University, Nagoya, Japan), respectively. Green fluorescent protein (GFP)-tagged Super-FAK (the K578E/K581E mutant) was provided by M. D. Schaller (University of North Carolina, Chapel Hill, NC) (15). HeLa S3 cells stably expressing h-prune (WT) or amino acid region 199 to 453 of h-prune [h-prune(199-453)] were generated by selection with G418. NIH 3T3 and HeLa S3 cells stably expressing GFP-paxillin were generated by selection with puromycin. The anti-Myc antibody was prepared from 9E10 cells. The anti-h-prune antibody was prepared in rabbits by immunization with recombinant h-prune(199-453) proteins. siRNA duplexes used were as follows: human GSK-3α (sense), 5′-GAAGGUUCUCC AGGACAAGTT-3′; human GSK-3β (sense), 5′-AGUUAGCAGAGACAAGG ACTT-3′; mouse GSK-3β (sense), 5′-GAAGUCUAGCCUAUAUCCATT-3′; h-prune (sense), 5′-GGCGUCAAGGUGGCCAUUATT-3′; and human casein kinase Iα (CKIα) (sense), 5′-CCAGGCAUCCCCAGUUGCUTT-3′. Other materials were from commercial sources.

Plasmid construction. pCGN/GSK-3β (WT), pCGN/GSK-3β K85M, pCGN/GSK-3β K85R, pCGN/GSK-3β Y216F, pCGN/GSK-3β S9A, and pGEX-4T/GSK-3β (WT) were constructed as previously described (21, 43). Standard recombinant DNA techniques were used to construct the following plasmids: pEF-BOS-Myc/h-prune (WT), pEF-BOS-Myc/h-prune(1-332), pEF-BOS-Myc/h-prune(199-453), pEF-BOS-Myc/h-prune(333-453), pGEX-6P/h-prune (WT), pV-IKS/h-prune (WT), pAd-CMV-Myc/h-prune (WT), and pRSETA/GSK-3β (WT).

Cell culture. COS, NIH 3T3, and HeLa S3 cells were grown in Dulbecco's modified Eagle's medium supplemented with 10% calf serum and 10% fetal bovine serum (FBS). C57MG cells were grown in Dulbecco's modified Eagle's medium supplemented with 10% FBS and 10 μg/ml insulin. SW480 and CHO cells were grown in RPMI medium and Ham's F-12 medium supplemented with 10% FBS, respectively. When necessary, the cells were treated with 3 to 10 μM SB216763 for 4 h or 10 to 30 mM LiCl for 12 h or transfected with the siRNA for GSK-3β or h-prune.

Cell migration assay. To measure the cell migration activity, Transwell and wound-healing assays were performed. The Transwell cell migration assay was performed using a modified Boyden chamber (tissue culture treated, 6.5-mm diameter, 10-μm thickness, 8-μm pores; Transwell) (Costar, Cambridge, MA) as described previously (20, 32). The haptotactic migration assay was done by coating only the lower surface of the polycarbonate membrane with 10 μg/ml collagen or fibronectin, whereas the random migration assay was done by coating both the upper and lower surfaces of the membrane with 0.1 μg/ml collagen. HeLa S3, SW480, and CHO cells (2.5×10^4 cells) and NIH 3T3 cells (2.5×10^5 cells) suspended in serum-free medium containing 0.1% bovine serum albumin with or without inhibitors were applied to the upper chamber and allowed to migrate to the lower side of the upper chamber for 2 to 12 h. The numbers of the cells that migrated to the lower side of the upper chamber were counted, and relative cell migration was expressed as the percentage of migrated cells with treatment compared to those without treatment.

To carry out the wound-healing assay, HeLa S3, C57MG, NIH 3T3, and SW480 cells were plated onto collagen- or fibronectin-coated coverslips. The monolayer cells were then scratched manually with a plastic pipette tip, and after being washed with phosphate-buffered saline, wounded monolayers of the cells were allowed to heal for 12 to 24 h.

Immunohistochemistry. The immunocytochemical analyses of the cultured cells were performed as described previously (51) except that the cultured cells were simultaneously fixed and permeabilized with phosphate-buffered saline containing 3.7% paraformaldehyde and 0.5% Triton X-100. The immunohistochemical analyses of paraffin-embedded tissues from patients were performed as previously described (30). The sections were counterstained with 0.1% hematoxylin. A result was considered positive when more than 50% of the cells were stained.

Clinicopathological analyses of h-prune. For immunohistochemical analyses, we used archival formalin-fixed, paraffin-embedded tissues from 134 patients who had undergone surgical excision for colorectal cancer (adenocarcinoma) ($n = 92$) or pancreatic cancer (ductal adenocarcinoma) ($n = 42$). Tumor staging was carried out according to the TNM staging system (40). The procedure to protect privacy was in accordance with the Ethical Guidelines for Human Genome/Gene Research enacted by the Japanese government. Correlations between clinicopathologic parameters and h-prune expression were analyzed by Fisher's exact test. *P* values less than 0.05 were considered statistically significant.

Live imaging of adhesion and lamellipodia. The dynamics of GFP-paxillin of the scratched monolayer cells were quantified as described previously (14, 46). Fluorescence intensities of individual adhesions from background-subtracted images were measured over time using MetaMorph software (Universal Imaging Corporation, Downingtown, PA). For rate constant measurements, periods of disassembly (decreasing fluorescence intensity) of adhesions containing GFP-paxillin were plotted on separate semilogarithmic graphs representing fluorescence intensity ratios over time. Semilogarithmic plots of fluorescence intensities as a function of time were generated using the formula $\ln (I_0/I)$ for disassembly, where I_0 is the initial fluorescence intensity and I is the fluorescence intensity at various time points. The slopes of linear regression trend lines fitted to the semilogarithmic plots were then calculated to determine apparent rate constants of disassembly. For each rate constant, measurements were made on at least 10 individual adhesions in five separate cells. For lamellipodium formation, images were captured at 5-min intervals for 60 min. The average area of protrusion (μm^2) per 5-min interval was calculated. Measurements were made with at least five separate cells (7).

Others. Yeast two-hybrid screening was carried out as previously described (21, 52). Immunoprecipitation assays and RNA interference (RNAi) were performed as described previously (18, 51). The GSK-3 activity was assayed by the use of synthetic peptides as substrates (21, 43). The PDE activity of HeLa S3 cells was assayed using [^{3}H]cAMP as a substrate (44). Activation of Rac was assayed using GST-CRIB (2).

RESULTS

Involvement of GSK-3 in cell migration. First, we examined the involvement of GSK-3 in cell motility using a Transwell migration assay. HeLa S3 cells migrated over both collagen and fibronectin (Fig. 1A). LiCl, which is known to inhibit GSK-3 activity (28, 42), reduced the migration of HeLa S3 cells, but NaCl did not affect the migration (Fig. 1A). SB216763, which is another GSK-3 inhibitor, also suppressed the migration (Fig. 1A). CHO cells migrated over fibronectin but not collagen, and LiCl reduced the migration (Fig. 1B). Overexpression of wild-type GSK-3β or a constitutively active form of GSK-3β did not affect cell migration (data not shown), indicating that GSK-3 is not a limiting factor for migration.

We depleted endogenous GSK-3 in HeLa S3 cells by RNAi to find whether GSK-3 is definitively involved in the regulation of cell migration. An siRNA for GSK-3β or GSK-3α reduced the respective levels but not the levels of vinculin and CKIα (Fig. 1C). A single-stranded sense oligonucleotide for GSK-3β or siRNA for CKIα did not affect the protein levels of GSK-3β and GSK-3α (Fig. 1C). A decrease of either GSK-3β or GSK-3α but not CKIα inhibited the migration of HeLa S3 cells (Fig. 1C). Since these assays were done by coating the lower surface of the membranes with substrates, these results indicate the involvement of GSK-3 in haptotaxis. Random migration was measured by coating both the upper and lower surfaces of the membrane with the substrates. Inhibition of GSK-3 also suppressed the random migration of HeLa S3 cells

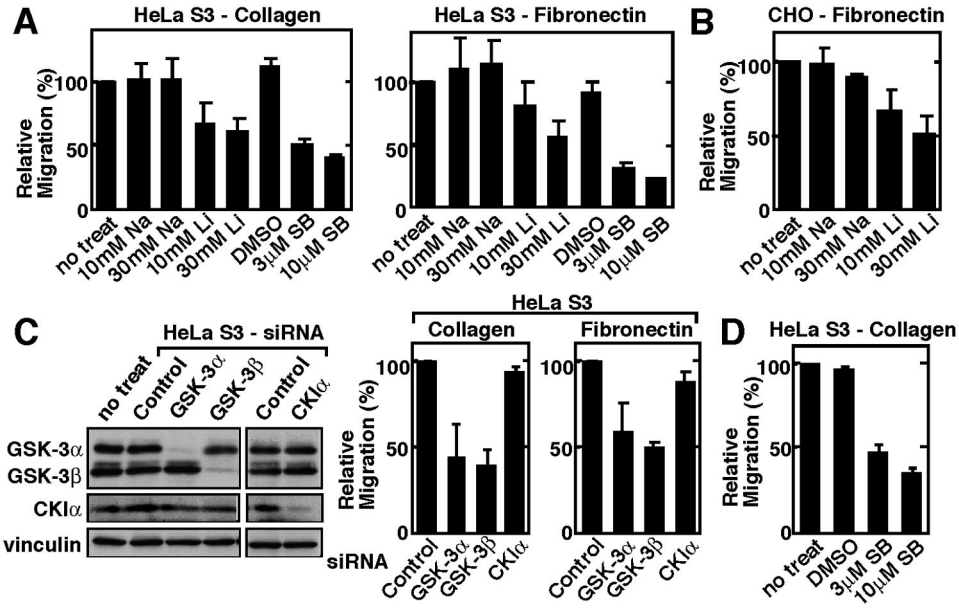

FIG. 1. Involvement of GSK-3 in cell migration. (A) HeLa S3 cells treated with the indicated inhibitors were subjected to the Transwell migration assay. (B) CHO cells treated with NaCl or LiCl were subjected to the Transwell migration assay. (C) Left panel, the lysates of HeLa S3 cells transfected with the indicated siRNAs were probed with the indicated antibodies. Right panel, HeLa S3 cells transfected with the indicated siRNAs were subjected to the Transwell migration assay. A single-strand RNA for GSK-3β was used as a control. (D) HeLa S3 cells treated with SB216763 were subjected to the random migration assay. The results shown are means ± standard errors of the means from four independent experiments. DMSO, dimethyl sulfoxide; Na, NaCl; Li, LiCl; SB, SB216763; no treat, no treatment.

(Fig. 1D). Therefore, GSK-3 is involved in both haptotactic and random migration. In the following experiments, we used a haptotactic assay. Inhibition of GSK-3 by LiCl in CHO cells and reduction of GSK-3β by RNAi in HeLa S3 cells did not inhibit cell adhesiveness (data not shown).

Identification of h-prune as a GSK-3-binding protein. To identify GSK-3-binding proteins that are involved in cell migration, we screened a human brain cDNA library using the yeast two-hybrid method. A 1.8-kb cDNA insert was found to carry a sequence containing an open reading frame for h-prune (Fig. 2A). h-prune belongs to the DHH family and exhibits PDE activity, and overexpression of h-prune enhances cell migration, which is inhibited by the suppression of its PDE activity (8).

Reciprocal immunoprecipitation analyses showed that GSK-3β and h-prune formed a complex at the endogenous level in HeLa S3 cells (Fig. 2B). GSK-3α also formed a complex with h-prune (Fig. 2B). In vitro binding studies using recombinant proteins demonstrated that GSK-3β bound directly to h-prune (Fig. 2C). Amino acid region 333 to 453 of h-prune was necessary and sufficient for the complex formation with GSK-3β in intact cells (Fig. 2D). Treatment of HeLa S3 cells with GSK-3 inhibitors decreased the formation of a complex between GSK-3β and h-prune (Fig. 2E). Furthermore, GSK-3β kinase-inactive mutants (the K85M, K85R, and Y216F mutants) did not form a complex with h-prune under the conditions in which wild-type GSK-3β and a constitutively active GSK-3β mutant (S9A) did (Fig. 2F). These results indicate that the kinase activity of GSK-3 is required for its interaction with h-prune in intact cells. GSK-3 did not phosphorylate h-prune in vitro, and SB216763 did not affect the phosphorylation of h-prune in intact cells, where ^{32}P was metabolically labeled (data not shown). h-prune does not possess the typical consensus sequences for phosphorylation by GSK-3. Therefore, it is unlikely that h-prune is a substrate of GSK-3.

The kinase activity of GSK-3 in the h-prune immune com-

FIG. 2. Interaction of h-prune with GSK-3. (A) Schematic representation of the deletion mutants of h-prune used in this study. (B) The lysates of HeLa S3 cells (lanes 1 and 6) were immunoprecipitated with anti-GSK-3β or anti-h-prune antibody, and the immunoprecipitates were probed with the indicated antibodies (lanes 3, 5, and 8). The immunoprecipitates formed with anti-Myc and anti-GFP antibodies were used as controls (lanes 2, 4, and 7). GSK-3α/β Ab is an antibody that recognizes both GSK-3α (α) and GSK-3β (β). (C) Recombinant His_6-GSK-3β, GST-h-prune, and GST (0.5 μg of protein) were stained with Coomassie brilliant blue (lanes 1 to 3). After 0.4 μM His_6-GSK-3β was incubated with 0.5 μM GST-h-prune or GST immobilized on glutathione-Sepharose in 100 μl of reaction mixture (20 mM Tris/HCl, pH 7.5, and 1 mM dithiothreitol) for 1 h at 4°C, GST-h-prune and GST were precipitated by centrifugation, and then the precipitates were probed with the anti-His_6 antibody (lanes 4 to 6). (D) The lysates of COS cells expressing the deletion mutants of Myc-h-prune were probed with anti-GSK-3β or anti-Myc antibody (lanes 1 to 5). The same lysates were immunoprecipitated with anti-Myc antibody, and the immunoprecipitates were probed with the indicated antibodies (lanes 6 to 10). (E) HeLa S3 cells treated with 10 μM SB216763 or 30 mM LiCl were lysed, and the lysates were probed with anti-GSK-3β or anti-h-prune antibody (lanes 1 to 4). The same lysates were immunoprecipitated with anti-GSK-3β (lanes 5 to 6) or anti-h-prune antibody (lanes 7 to 10), and the immunoprecipitates were probed with the indicated antibodies. The lower bands detected by anti-h-prune antibody in Fig. 2B

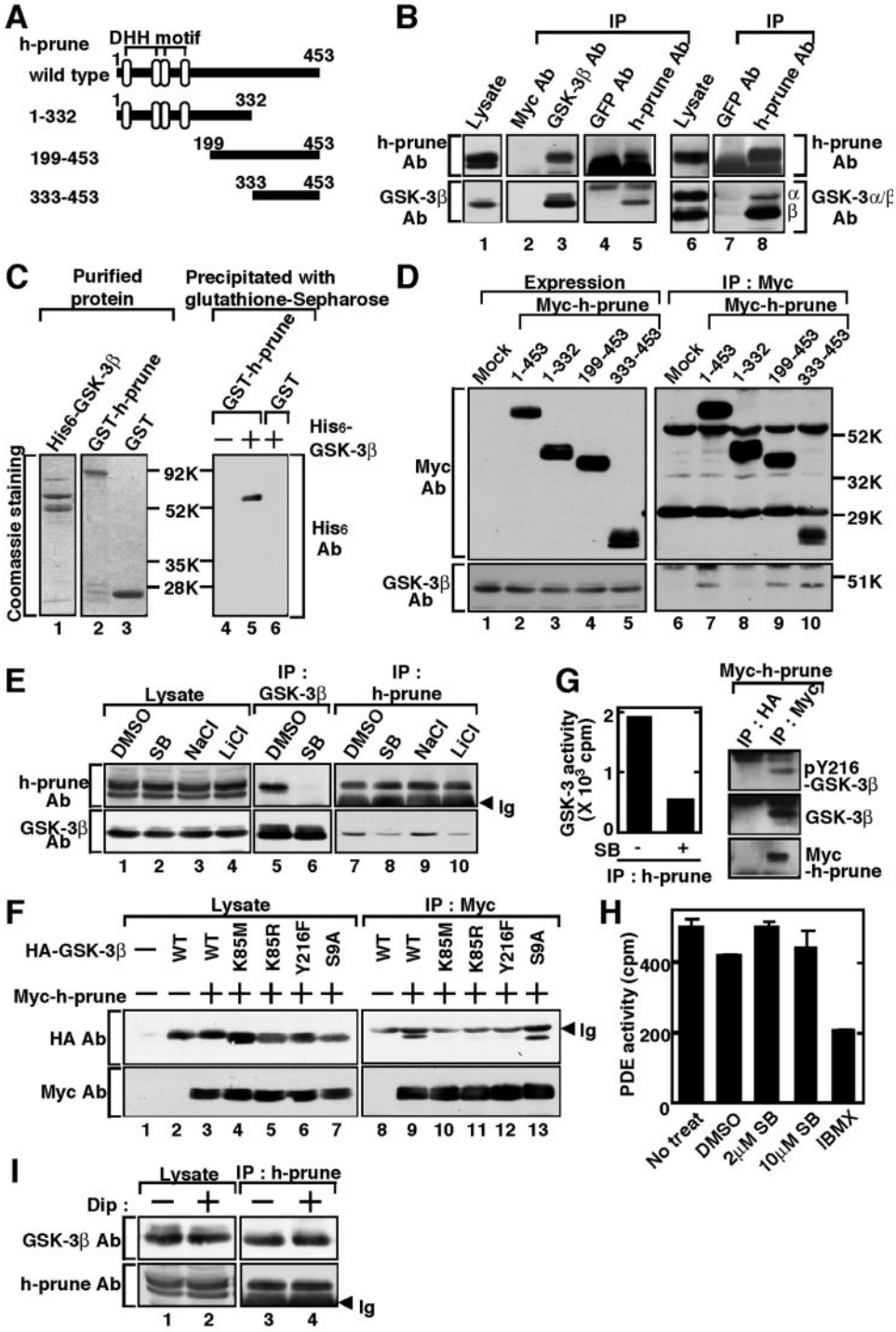

and E are nonspecific bands. (F) The lysates of COS cells expressing HA–GSK-3β mutants and Myc-h-prune were probed with anti-HA or anti-Myc antibody (lanes 1 to 7). The same lysates were immunoprecipitated with anti-Myc antibody, and the immunoprecipitates were probed with the indicated antibodies (lanes 8 to 13). (G) Left panel, the kinase activity of GSK-3 in the immunoprecipitates from HeLa S3 cells with anti-h-prune antibody was measured in the presence or absence of SB216763 in vitro. Right panel, the lysates of HeLa S3 cells expressing Myc-h-prune were immunoprecipitated with anti-Myc or anti-HA antibody, and the immunoprecipitates were probed with anti-GSK-3β antibody and the phospho-specific antibody to GSK-3β Tyr216 (pY216-GSK-3β). (H) The PDE activity of h-prune in HeLa S3 cells was measured after treatment with SB216763 in intact cells or with IBMX in vitro. (I) After HeLa S3 cells were treated with 10 μM dipyridamole for 4 h, h-prune was immunoprecipitated from the lysates and the immunoprecipitates were probed with anti-GSK-3β and anti-h-prune antibodies. HA, hemagglutinin; IP, immunoprecipitation; Ab, antibody; SB, SB216763; Dip, dipyridamole; Ig, immunoglobulin; DMSO, dimethyl sulfoxide; no treat, no treatment; Mock, control.

plexes was detected using peptide substrates, and the Tyr216-phosphorylated form of GSK-3β, which is an active form, was observed in the h-prune immune complexes (Fig. 2G), indicating that GSK-3 complexed with h-prune is active. The PDE activity in the h-prune immune complexes from HeLa S3 cells expressing h-prune was measured using [^{3}H]cAMP as a substrate. This activity was indeed inhibited by 3-isobutyl-1-methylxanthine (IBMX), a well-known PDE inhibitor. However, the PDE activity was not affected by the treatment of HeLa S3 cells with GSK-3 inhibitors (Fig. 2H). Therefore, the kinase activity of GSK-3 is not required for the PDE activity of h-prune. Dipyridamole was shown to inhibit the PDE activity (8). Treatment of HeLa S3 cells with dipyridamole did not affect the complex formation between h-prune and GSK-3β (Fig. 2I), suggesting that the PDE activity of h-prune is not necessary for the binding of h-prune to GSK-3.

Involvement of h-prune in cell migration. An siRNA for h-prune suppressed cell motility in the Transwell migration assay (Fig. 3A), indicating that h-prune is necessary for cell migration. Expression of the C-terminal region of Myc-h-prune in HeLa S3 cells inhibited the formation of a complex of GSK-3β with h-prune at the endogenous levels, and the cells expressing the Myc-h-prune mutant (C1 and C33) exhibited slow migration (Fig. 3B). These results suggest that the binding of GSK-3 and h-prune is involved in cell migration.

Localization of h-prune to focal adhesions. To clarify the mode of regulation of cell migration by GSK-3 and h-prune, the subcellular localization of these proteins was examined. GSK-3β was observed to be localized along with stress fibers in HeLa S3 cells when the cells were treated with 0.5% Triton X-100 to remove soluble proteins (Fig. 4A, a to c). h-prune was located at focal adhesions at the cell bottom, where paxillin was present, and these two proteins were colocalized (Fig. 4A, d to f). Similar subcellular localizations of these two proteins were also observed in C57MG mouse mammary gland cells (Fig. 4B, a to c and m to o). GSK-3β was located to stress fibers, and GSK-3β on the ends of stress fibers was colocalized with paxillin at focal adhesions (Fig. 4B, a to f). Furthermore, the Tyr216-phosphorylated form of GSK-3β was present at the terminal regions of stress fibers (Fig. 4B, g to i), consistent with previous observations (3). h-prune was observed on the ends of stress fibers at focal adhesions and colocalized with paxillin (Fig. 4B, j to o). h-prune and GSK-3 were partially colocalized to the ends of stress fibers at focal adhesions (Fig. 4B, p to r). h-prune and vinculin, another focal adhesion protein, were also clearly colocalized to focal adhesions at the cell bottom (data not shown). Consistent with these results, immunoprecipitation assays demonstrated that h-prune is associated with paxillin and vinculin in addition to GSK-3β at the endogenous levels in HeLa S3 (data not shown) and C57MG (Fig. 4C) cells. Myc-h-prune(1-332) but not Myc-h-prune(333-453) or Myc-h-prune(199-453) interacted with paxillin (Fig. 4D), indicating that GSK-3 and paxillin form a complex with different regions of h-prune. Furthermore, recombinant GST-paxillin precipitated h-prune, vinculin, and GSK-3β from the HeLa S3 cells expressing Myc-h-prune (Fig. 4E). Taken together, these results suggest that h-prune links active GSK-3 to focal adhesions.

Involvement of GSK-3 and h-prune in formation of focal adhesions. The scratch wound migration assay was performed

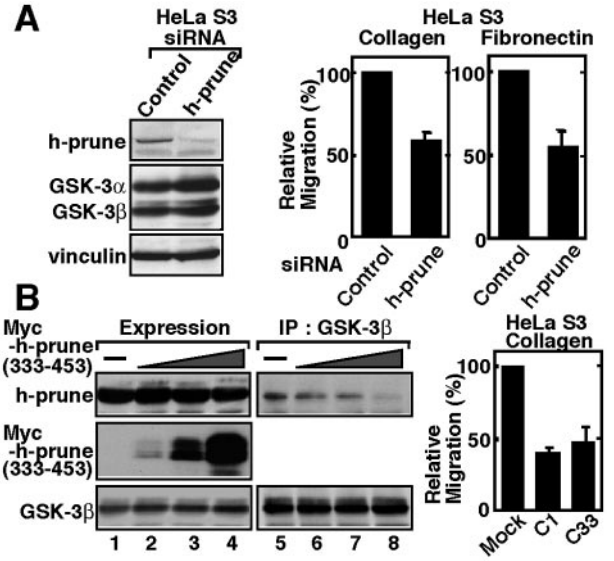

FIG. 3. Involvement of h-prune in cell migration. (A) Left panel, the lysates of HeLa S3 cells transfected with control siRNA or siRNA for h-prune were probed with the indicated antibodies. Right panel, HeLa S3 cells transfected with control siRNA or siRNA for h-prune were subjected to the Transwell migration assay. (B) Left panel, the lysates of HeLa S3 cells expressing Myc-h-prune(333-453) were probed with anti-h-prune or anti-GSK-3β antibody (lanes 1 to 4). The same lysates were immunoprecipitated with anti-GSK-3β antibody (lanes 5 to 8). Right panel, two different clones (C1 and C33) of HeLa S3 cells stably expressing Myc-h-prune(199-453) were subjected to the Transwell migration assay. Cells transfected with vectors alone were used as a control (Mock). The results shown are means ± standard errors of the means from three independent experiments. IP, immunoprecipitation.

to examine the roles of GSK-3 and h-prune in the formation of focal adhesions. C57MG cells were allowed to migrate in scratch wound cultures, resulting in wound closure after 12 h, which was inhibited by SB216763 (Fig. 5A). Paxillin and vinculin were observed clearly in control migrating cells, and h-prune was colocalized with them (Fig. 5B, a to c and j to l). Large focal adhesions, including paxillin, vinculin, and h-prune, were formed at a leading edge of the cells treated with SB216763 (Fig. 5B, d to f, m to o). These proteins seemed to be accumulated at focal adhesions in the treated cells compared with control cells. Dipyridamole did not affect the subcellular localization of paxillin and h-prune (Fig. 5B, g to i), indicating that the PDE activity is not required for the localization of h-prune to focal adhesions. h-prune accumulated in the cells treated with SB216763 was localized to the tips of actin fibers (data not shown). To perform similar experiments with RNAi, we analyzed HeLa S3 cells. At the cell front along the leading edge of migrating HeLa S3 cells, weak staining of paxillin and vinculin was detected and little h-prune was observed (Fig. 5C, a to c and g to i). GSK-3β knocked-down cells exhibited the accumulation of paxillin, vinculin, and h-prune at focal adhesions (Fig. 5C, d to f and j to l).

Inhibition of GSK-3 activity did not affect the expression level of h-prune (Fig. 2E). Since it has been suggested that the formation of large focal adhesions is due to the reduced turnover of adhesions (36), the effects of GSK-3 and h-prune on

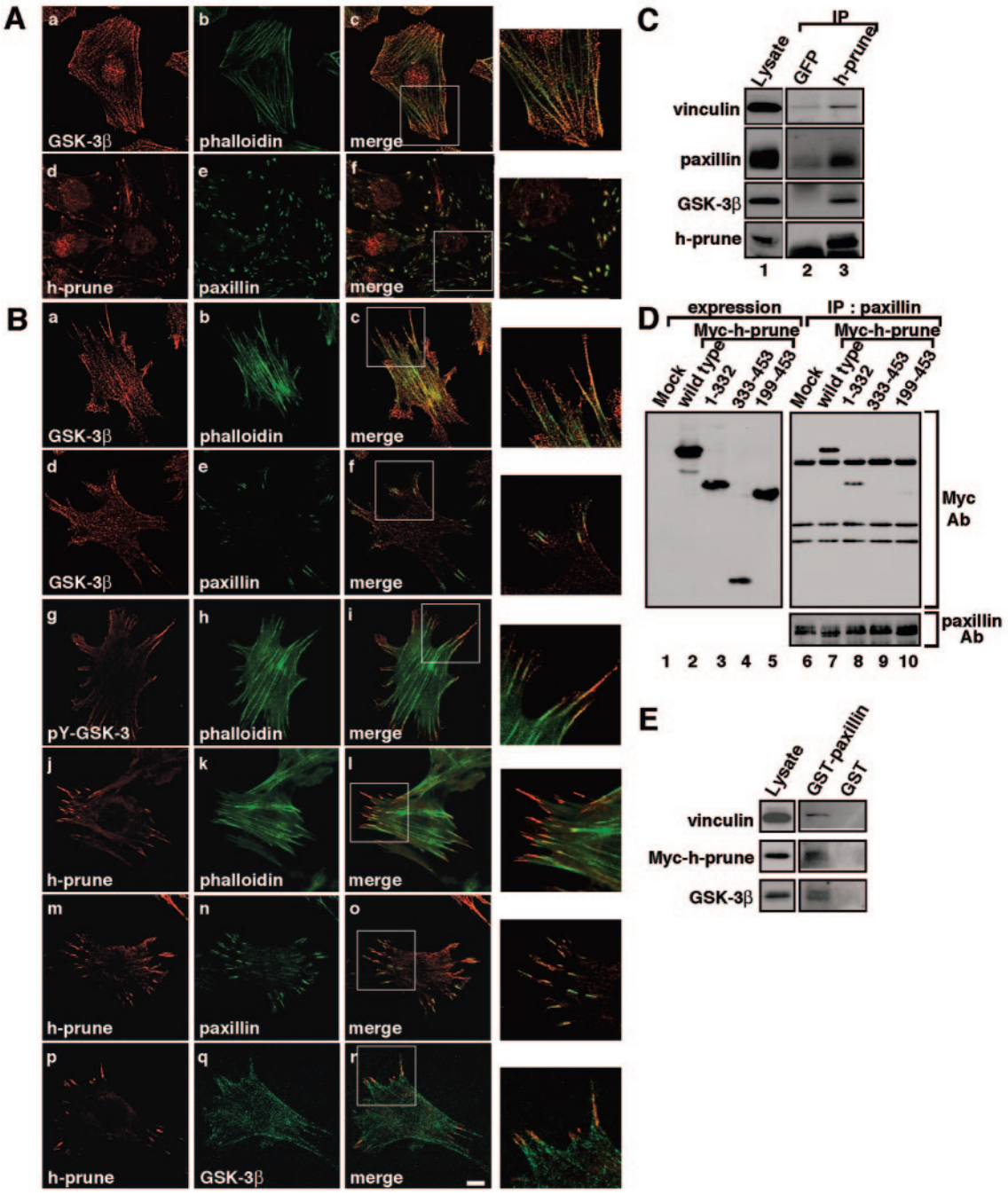

FIG. 4. Localization of h-prune and GSK-3 to focal adhesions. (A) HeLa S3 cells were stained with anti-GSK-3β (a), anti-h-prune (d), or antipaxillin (e) antibody or phalloidin-fluorescein isothiocyanate (FITC) (b). Merged images are shown in panels c and f. The regions in white boxes are shown magnified. (B) C57MG cells were stained with anti-GSK-3β (a and d), anti-pY216-GSK-3β (g), anti-h-prune (j, m, and p), or antipaxillin (e and n) antibody or phalloidin-FITC (b, h, and k). To show the localization of GSK-3 and h-prune simultaneously, anti-GSK-3 antibody was labeled with a Zenon labeling kit (Molecular Probes) (q). Merged images are shown in panels c, f, i, l, o, and r. The regions in white boxes are shown magnified. Scale bar, 10 μm. (C) The lysates of C57MG cells (lane 1) were immunoprecipitated with anti-h-prune antibody, and the immunoprecipitates were probed with the indicated antibodies (lane 3). The immunoprecipitates obtained with anti-GFP antibody were used as a control (lane 2). (D) The lysates of COS cells expressing deletion mutants of h-prune were probed with anti-Myc antibody (lanes 1 to 5). The same lysates were immunoprecipitated with antipaxillin antibody, and the immunoprecipitates were probed with the indicated antibodies (lanes 6 to 10). The results shown are representative of three independent experiments. (E) HeLa S3 cells expressing Myc-h-prune were lysed, and the lysates were incubated with 0.1 μM GST-paxillin or GST immobilized on glutathione-Sepharose. After GST-paxillin or GST was precipitated by centrifugation, the precipitates were probed with the indicated antibodies. IP, immunoprecipitation; Ab, antibody; Mock, control.

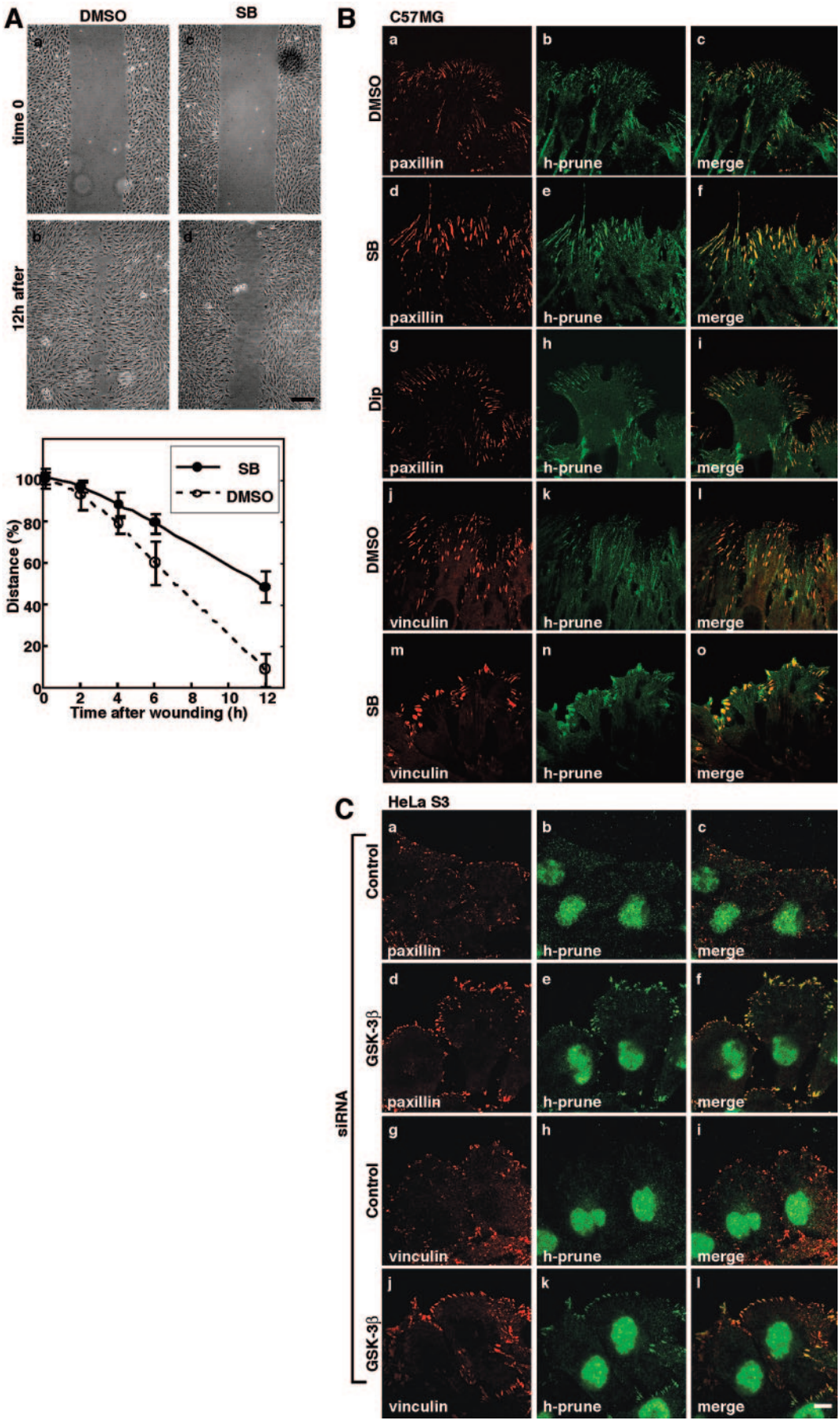

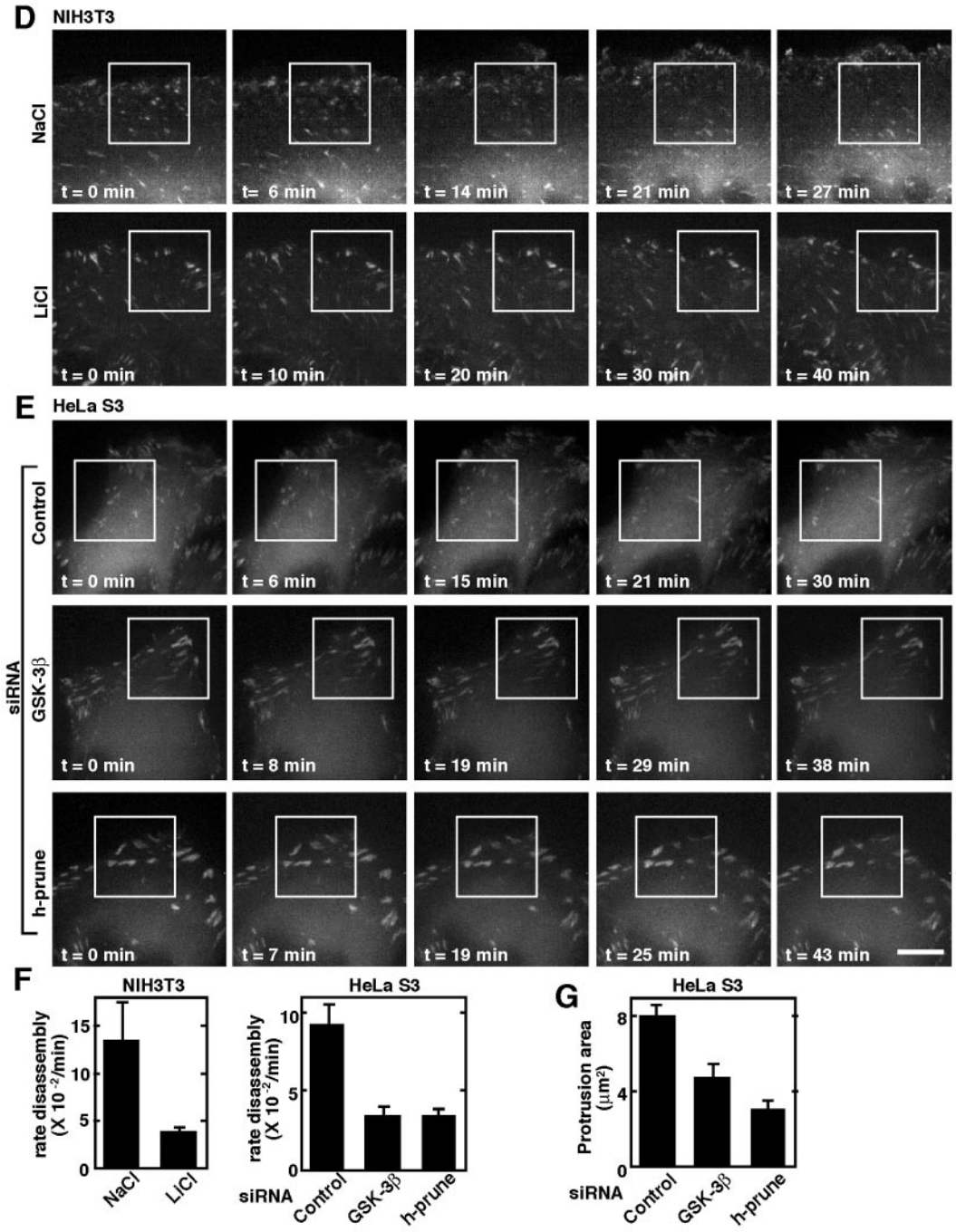

FIG. 5. Involvement of GSK-3 and h-prune in dynamics of focal adhesions. (A) Upper panel, monolayers of C57MG cells on collagen-coated coverslips were treated with 10 μM SB216763 for 4 h. After wounding, wounded monolayers were allowed to heal for 12 h. Scale bar, 0.2 mm. Lower panel, the length of the wounds was measured and expressed as a percentage of the initial distance at time zero. Open circles, dimethyl sulfoxide (DMSO) treatment; filled circles, SB216763 (SB) treatment. The results shown are means ± standard errors of the means from three independent experiments. (B) C57MG cells treated with 10 μM SB216763 (d to f, m to o) or 10 μM dipyridamole (Dip) (g to i) were wounded. Six hours after wounding, the cells were stained with antipaxillin (a, d, and g), antivinculin (j and m), or anti-h-prune (b, e, h, k, and n) antibody. Merged images are shown in panels c, f, i, l, and o. (C) HeLa S3 cells transfected with the siRNA for GSK-3β (d to f and j to l) were wounded. Twelve hours after wounding, the cells were stained with antipaxillin (a and d), antivinculin (g and j), or anti-h-prune (b, e, h, and k) antibody. Merged images are shown in panels c, f, i, and l. Scale bar, 10 μm. The results shown are representative of three independent experiments. (D and E) Dynamics of GFP-paxillin in migrating NIH 3T3 cells treated with NaCl or LiCl (D) and those in HeLa S3 cells treated with the indicated siRNAs (E) were visualized by time-lapse fluorescence microscopy. For each sequence, "t = 0 min" is the frame in which the adhesions in the white box were clearly observed. Scale bar, 5 μm. (F) Rate constants for disassembly of GFP-paxillin in Fig. 5D and E were calculated. Quantifications of GFP-paxillin disassembly show means ± standard errors of the means. (G) The lamellipodium protrusion area was quantified in HeLa S3 cells transfected with siRNA for GSK-3β or h-prune.

the dynamics of focal adhesions were examined. We expressed GFP-paxillin in NIH 3T3 and HeLa S3 cells and analyzed the turnover of adhesions by live fluorescence imaging. At the cell front, paxillin-containing adhesions disassembled as new adhesions were formed near the leading edge (47). We measured the rate constant of disassembly of paxillin-containing adhesions in migrating NIH 3T3 cells and found that the average rate of disassembly of GFP-paxillin from adhesion sites was decreased in LiCl-treated cells (Fig. 5D and F) (see Video S1 in the supplemental material). The rate constants of disassembly of paxillin in NaCl-treated and LiCl-treated cells were $(13.5 \pm 4) \times 10^{-2}\ \mathrm{min}^{-1}$ and $(3.9 \pm 0.4) \times 10^{-2}\ \mathrm{min}^{-1}$, respectively. We also found that the average rate of disassembly of GFP-paxillin was reduced in the GSK-3β or h-prune knocked-down cells (Fig. 5E and F) (see Video S2 in the supplemental material). The rate constants of disassembly of paxillin in control RNA-treated cells, GSK-3β knocked-down cells, and h-prune knocked-down cells were $(9.3 \pm 1.4) \times 10^{-2}\ \mathrm{min}^{-1}$, $(3.4 \pm 0.6) \times 10^{-2}\ \mathrm{min}^{-1}$, and $(3.4 \pm 0.5) \times 10^{-2}\ \mathrm{min}^{-1}$, respectively. Lamellipodia at cell fronts were quantified by measuring the area of protrusion. Lamellipodium protrusion formation was reduced in GSK-3β or h-prune knocked-down cells (Fig. 5G). Taken together, these results suggest that both GSK-3 and h-prune are necessary for the efficient disassembly of adhesion complexes.

Involvement of GSK-3 and h-prune in activation of FAK and Rac. It has been reported that fibroblasts lacking FAK have a reduced migration rate, with an increase in the number and size of peripherally localized adhesions (22, 46). Several tyrosine residues become phosphorylated upon FAK activation (34, 50). FAK is activated via autophosphorylation at Tyr397, which is initiated by integrin engagement with its ligand (38). Therefore, to examine the roles of GSK-3 and h-prune in the activation of FAK, integrin was activated by attaching HeLa S3 cells to collagen. Phosphorylation of Tyr397 of FAK by stimulation with collagen was decreased in GSK-3β and h-prune knocked-down cells (Fig. 6A). Overexpression of h-prune(199-453), which inhibits the interaction of GSK-3 with h-prune, also suppressed the phosphorylation of Tyr397 of FAK (Fig. 6B). These results suggest that FAK acts downstream of GSK-3. Consistent with these observations, expression of $FAK^{K578E/K581E}$, a constitutively active form of FAK (15), partially rescued the inhibition of migration in GSK-3β knocked-down cells (Fig. 6C). We next examined the roles of GSK-3 and h-prune in the activation of the small G protein Rac, which stimulates cell migration. Collagen-dependent activation of Rac was suppressed by reducing GSK-3β and h-prune in HeLa S3 cells or by inhibiting GSK-3 activity (Fig. 6C). Rac was activated by scratch wound, and this scratch-induced Rac activation was also suppressed in HeLa S3 cells treated with SB216763 (Fig. 6E). Taken together, these results suggest that GSK-3 and h-prune regulate the activation of FAK and Rac cooperatively.

Correlation of h-prune expression with tumor aggressiveness. h-prune has been reported to be highly expressed in breast cancer (8, 55). We verified the expression of h-prune in other tumors, such as colorectal and pancreatic cancers. Although nonneoplastic colorectal epithelium contained some h-prune-positive cells, cancer tissue gave stronger and more extensive staining (Fig. 7A, a and b). Results were considered positive when more than 50% of the cells were stained. In total, 27 (29.3%) of 92 colorectal cancer cases were positive for h-prune. The positivity of h-prune was correlated with the advanced T grade (depth of invasion), N grade (degree of lymph node metastasis), and M grade (distant metastasis) ($P = 0.0132$, $P = 0.0044$, and $P = 0.0215$, respectively; Fisher's exact test) (Table 1). Moreover, h-prune staining was observed more frequently in stage III/IV cases than in stage I/II cases ($P = 0.0044$). Similar findings were also observed in the cases of pancreatic cancer (18/42 cases were positive) except for M grade cases (Fig. 7A, c and d, and Table 2). There was no significant association between h-prune expression and M grade, but pancreatic cancer cases with distant metastasis had a tendency to express h-prune more strongly than those without distant metastasis. These findings suggest that highly expressed h-prune could be generally related to higher tumor aggressiveness.

As seen in other cell lines, h-prune was colocalized with paxillin at focal adhesions in SW480 colorectal cancer-derived cells (Fig. 7B). In scratch wound culture, treatment of SW480 cells with SB216763 or the siRNA for GSK-3β or h-prune caused the accumulation of paxillin at the leading edge (Fig. 7C). Reduction of GSK-3 or h-prune by RNAi inhibited the migration of SW480 cells (Fig. 7D). Consistent with previously reported observations (8), dipyridamole suppressed the migration of SW480 cells (Fig. 7E). Furthermore, SB216763 and dipyridamole inhibited cell migration additively (Fig. 7E), suggesting that the combination of the inhibitors for the h-prune PDE activity and GSK-3 kinase activity prevents invasiveness or metastasis of colorectal cancer.

DISCUSSION

Cell migration is a complex cellular behavior that involves protrusion and adhesion at the cell front and contraction and detachment at the rear (36). In this study, we provide evidence that GSK-3 and h-prune regulate cell migration cooperatively. Treatment of the cells with GSK-3 inhibitors induced the dissociation of GSK-3 from h-prune and suppressed cell migration. Knockdown of GSK-3 or h-prune by RNAi also inhibited cell migration. Furthermore, expression of the C-terminal region of h-prune in HeLa S3 cells inhibited the interaction of GSK-3 with h-prune and cell migration. Although we cannot exclude the possibility that overexpression of the C-terminal region of h-prune has other effects, these results suggest that the binding of GSK-3 to h-prune is necessary for cell migration. Furthermore, inhibition of GSK-3 affected both haptotactic and random migration. It has been suggested that haptotactic migration is more dependent on the ability of cells to form adhesive contacts at the cell front and that random migration is more limited by the ability of cells to release adhesions at the cell rear (20). Therefore, GSK-3 plays a role in the assembly and/or disassembly of focal adhesions.

How do GSK-3 and h-prune regulate cell motility? GSK-3 or h-prune knocked-down cells exhibited large focal adhesions. Furthermore, reduction of GSK-3 or h-prune by RNAi impaired the disassembly of paxillin from focal adhesions. Similar phenotypes of abnormal focal adhesions with reduced cell migration are observed in the fibroblasts from mice lacking FAK (22). FAK activation, demonstrated by an increase in the phosphorylation of Tyr397 in the protein, is best understood in the

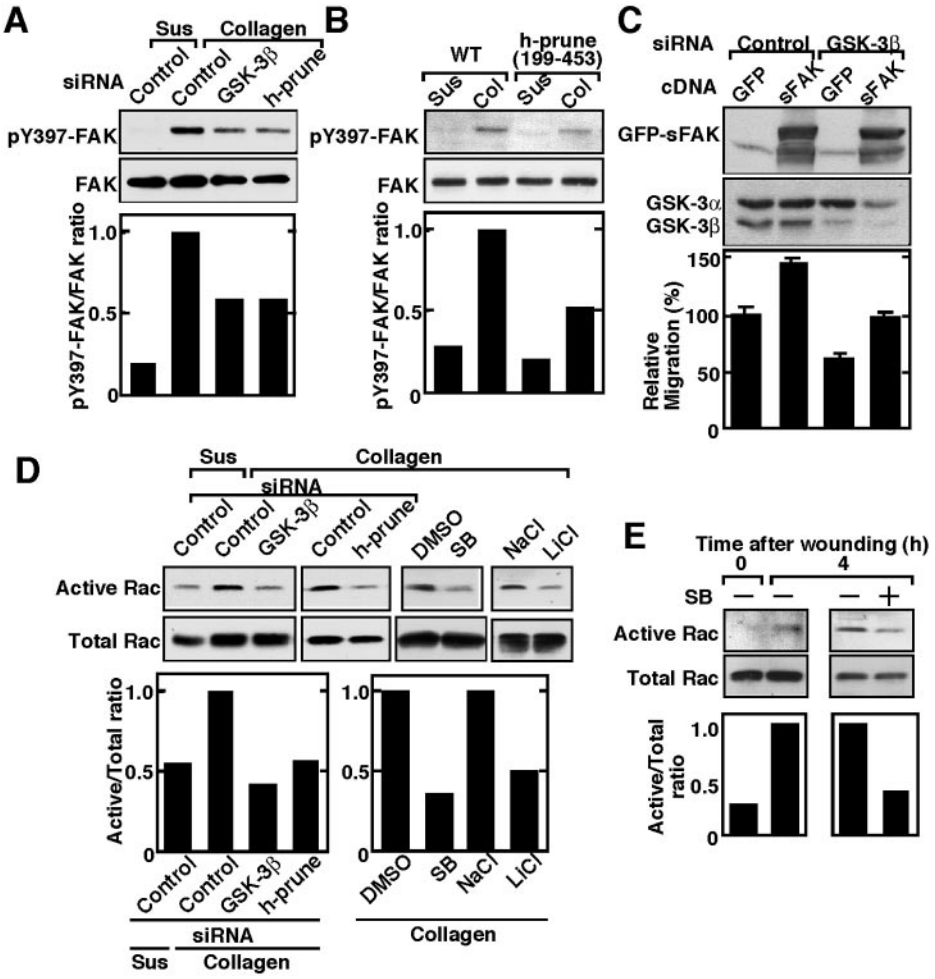

FIG. 6. Involvement of GSK-3 and h-prune in the activation of FAK and Rac. (A and B) FAK activation. HeLa S3 cells transfected with the indicated siRNAs (A) or expressing Myc-h-prune(199–453) (B) were suspended in serum-free medium and were kept in suspension (Sus) or replated onto collagen-coated dishes (Col). Top panel, the cells were lysed at 1 h after plating, and the lysates were probed with the phospho-specific antibody to FAK pTyr397 (pY397 FAK) or anti-FAK antibody. Bottom panel, the FAK activity was measured as the ratio of phosphorylated FAK (active FAK) to total FAK. (C) GFP or GFP-FAK$^{K578E/K581E}$ (sFAK) was expressed in NIH 3T3 cells transfected with siRNA for GSK-3β, and the cells were subjected to the Transwell migration assay. Migrated GFP-labeled cells were normalized with transfection efficiency. Top panel, the protein levels of GFP-FAK$^{K578E/K581E}$ and GSK-3β were shown by anti-FAK and GSK-3 antibodies. Bottom panel, migration ability of the cells used in this assay. (D) Rac activation. HeLa S3 cells were transfected with the indicated siRNAs or treated with the indicated GSK-3 inhibitors. The cells were replated onto collagen-coated dishes, and the lysates were incubated with GST-CRIB immobilized on glutathione-Sepharose. Top panel, the total lysates and precipitates were probed with anti-Rac-1 antibody. Bottom panel, the Rac activity was measured as the ratio of the amount of CRIB-bound Rac (active Rac) to that of Rac in total cell lysates (total Rac). (E) Multiple wounds were made several times in HeLa S3 cells treated with 10 μM SB216763 (SB). The Rac activity was measured at 4 h after wounding. DMSO, dimethyl sulfoxide.

context of the engagement of integrins at the cell surface (34). Activation of FAK results in the recruitment of a number of SH2-domain- and SH3-domain-containing proteins. Among them, p130Cas and Crk are involved in cell migration (34). Dominant negative Rac blocks the increased migration in response to the expression of p130Cas and Crk, probably through DOCK180, which suggests that Rac is an important downstream effector of the FAK-Cas-Crk complex.

We showed that the phosphorylation of Tyr397 in FAK and the activation of Rac induced by collagen are reduced in the GSK-3 or h-prune knocked-down cells. Furthermore, treatment with GSK-3 inhibitors or overexpression of the C-terminal region of h-prune also showed the same results as those obtained in the GSK-3 or h-prune knocked-down cells. It has been demonstrated that FAK plays a prominent role in integrin signaling and that Rac is required for adhesion turnover (34, 39). Therefore, FAK and Rac could act downstream of GSK-3 and h-prune. Consistent with these observations, expression of a constitutively active form of FAK rescued the inhibition of cell migration in GSK-3 knocked-down cells although it was partial. The phosphorylation of proteins by GSK-3 at focal adhesions may be required to mediate the integrin signal. The substrates of GSK-3 that regulate FAK activity remain to be identified.

Several reports have shown that GSK-3 negatively regulates cell migration. For example, integrin inhibits GSK-3 through the activation of integrin-linked kinase and PKB/Akt, and activation of PKB/Akt promotes cell migration (26). Further-

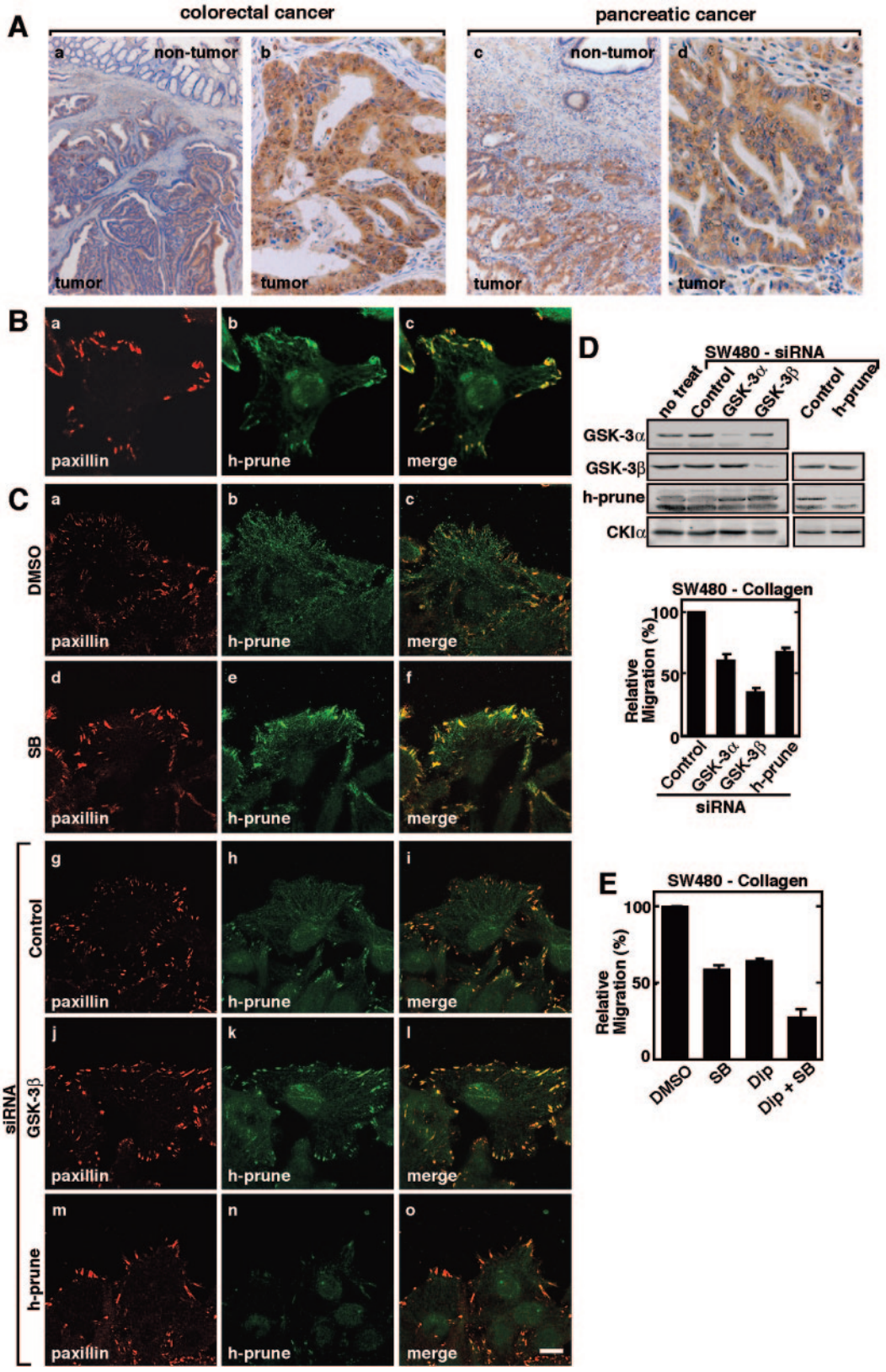

FIG. 7. Correlation of h-prune expression with tumor aggressiveness. (A) Immunohistochemical analyses of h-prune in human colorectal cancer (a and b) and human pancreatic cancer (c and d). (a) Magnification, ×13; (c) magnification, ×33. Expression levels of h-prune in the nontumor and tumor regions were compared. (b and d) Magnification, ×135. The tumor regions were enlarged. (B) SW480 cells were stained with antipaxillin (a) or anti-h-prune (b) antibody. The merged image is shown in panel c. (C) SW480 cells treated with 10 μM SB216763 (d to f) or transfected with the siRNA for GSK-3β (j to l) or h-prune (m to o) were wounded. Twelve hours after wounding, the cells were stained with antipaxillin

TABLE 1. Relation between h-prune expression and clinicopathologic characteristics in colorectal cancer

Characteristic[a]	No. of cases (%) with indicated h-prune expression		*P* value
	Positive	Negative	
T grade			
T1/2	3 (11.1)	24	0.0132
T3/4	24 (36.9)	41	
N grade			
N0	10 (17.9)	46	0.0044
N1/2	17 (47.2)	19	
M grade			
M0	22 (25.9)	63	0.0215
M1	5 (71.4)	2	
Stage			
I/II	10 (17.9)	46	0.0044
III/IV	17 (47.2)	19	

[a] T1, tumor invades submucosa; T2, tumor invades muscularis propria; T3, tumor invades through muscularis propria into subserosa or into nonperitonealized pericolic or perirectal tissue; T4, tumor directly invades other organs or structures and/or perforates visceral peritoneum. N0, no regional lymph node metastasis; N1, metastasis in one to three regional lymph nodes; N2, metastasis in four or more regional lymph nodes. M0, no distant metastasis; M1, distant metastasis.

TABLE 2. Relation between h-prune protein expression and clinicopathologic characteristics in pancreatic cancer

Characteristic[a]	No. of cases (%) with indicated h-prune expression		*P* value
	Positive	Negative	
T grade			
T1/2	2 (15.4)	11	0.0208
T3/4	16 (55.2)	13	
N grade			
N0	5 (25.0)	15	0.0334
N1	13 (59.1)	9	
M grade			
M0	10 (35.7)	18	0.2079
M1	8 (57.1)	6	
Stage			
I/II	10 (35.7)	18	0.2079
III/IV	8 (57.1)	6	

[a] T1, tumor limited to pancreas (2 cm or less in greatest dimension); T2, tumor limited to pancreas (more than 2 cm in greatest dimension); T3, tumor extends beyond pancreas but without involvement of celiac axis or superior mesenteric artery; T4, tumor invades celiac or superior mesenteric artery. N0, no regional lymph node metastasis; N1, regional lymph node metastasis. M0, no distant metastasis; M1, distant metastasis.

more, PKB/Akt promotes integrin recycling by inactivating GSK-3 (37), and hypoxia-induced tumor cell invasion is mediated by inhibiting GSK-3 (53). However, inhibition of GSK-3 has been demonstrated to prevent the accumulation of Rac at lamellipodia and to inhibit epidermal growth factor-dependent wound closure (29), consistent with our results showing that GSK-3 positively regulates cell migration. Although the exact reasons for the differences between our results and those of others are not known, it has been demonstrated that GSK-3 is rapidly and transiently activated, followed by its inhibition by extracellular stimuli, including insulin and epidermal growth factor, or cell adhesion (6, 31). Therefore, cell migration may involve cyclic transient activation and inactivation of GSK-3 as well as modulation of the cellular localization of GSK-3. Since our results suggest that GSK-3 forms a complex with focal adhesions through h-prune, the GSK-3 activity may be necessary to trigger the integrin signal. Another possibility is that GSK-3 binds to h-prune at a site other than focal adhesion. In this model, when GSK-3 is inactivated by integrin, h-prune dissociates from GSK-3 and locates to focal adhesions. Then, h-prune may promote cell migration with GSK-3 after the kinase activity is recovered.

We showed that h-prune overexpression in colorectal and pancreatic cancers is correlated with the depth of invasion and the degree of lymph node metastasis. Taken together with the observations that h-prune is highly expressed in invasive breast cancer (55), this suggests that h-prune might be used as a marker for the identification of subsets of the cancer patients with higher tumor aggressiveness. h-prune has cyclic nucleotide PDE activity, and inhibition of the PDE activity by dipyridamole suppresses cell motility (8). Although a correlation between an h-prune PDE activity and cellular motility has been shown, GSK-3 did not affect the PDE activity of h-prune. Inhibition of GSK-3 and h-prune additively suppressed the cell migration of colon cancer cells, suggesting that h-prune regulates cell motility by two different actions through the PDE activity and the GSK-3 binding activity. Therefore, the identification of highly specific inhibitors of GSK-3 and h-prune might be useful for developing medicines to prevent or treat cancer metastasis.

It has been reported that *Drosophila* prune genetically interacts with $awd^{k\text{-}pn}$, which encodes a nucleotide diphosphate kinase as well as mammalian nm23-H1 (4), and that h-prune and nm23-H1 protein levels are unbalanced in sarcoma and breast cancers (12), suggesting that h-prune may negatively regulate nm23-H1 antimetastatic activity. These results are consistent with the previous observations that nm23-H1 is downregulated in certain cancer cells with high metastasis (33). However, the expression levels of nm23-H1 show no relationship with metastasis of other cancer cells, such as colorectal cancer (17). Since we could not detect the presence of nm23-H1 in the GSK-3 immune complexes (data not shown), whether the complex of GSK-3, h-prune, and nm23-H1 is present and whether this ternary complex is involved in cell migration are not known.

Protein complexes containing GSK-3 regulate the functions of GSK-3 in different subcellular locations. Frat-1, which is known to be involved in the regulation of β-catenin stability, binds to GSK-3 and facilitates its nuclear export (13). p53 interacts with GSK-3 in the nucleus. This association activates

(a, d, g, j, and m) or anti-h-prune (b, e, h, k, and n) antibody. Merged images are shown in panels c, f, i, l, and o. Scale bar, 10 μm. (D) Upper panel, the lysates of SW480 cells transfected with the indicated siRNAs were probed with the indicated antibodies. Lower panel, SW480 cells transfected with the indicated siRNAs were subjected to the Transwell migration assay. (E) SW480 cells treated with 10 μM SB216763 and/or 10 μM dipyridamole were subjected to the Transwell migration assay on collagen. SB, SB216763; Dip, dipyridamole; DMSO, dimethyl sulfoxide. The results shown are means ± standard errors of the means from three independent experiments.

GSK-3, and GSK-3 promotes the transcriptional and apoptotic actions of p53 (45). Further studies to identify additional GSK-3-binding proteins will be necessary to clarify how regulatory mechanisms are integrated to achieve substrate-specific regulation of GSK-3 activity.

ACKNOWLEDGMENTS

We are grateful to K. Matsumoto, S. Takada, J. R. Woodgett, Y. Matsuura, H. Sabe, K. Kaibuchi, and M. D. Schaller for donating cells, plasmids, and baculoviruses.

This work was supported by Grants-in-Aid for Scientific Research and for Scientific Research on Priority Areas from the Ministry of Education, Science, and Culture, Japan (2002, 2003, 2004, 2005); by grants from the Yamanouchi Foundation for Research on Metabolic Disorders (2003) and the Sankyo Foundation of Life Science (2004, 2005); and by grants from EU FP6-BRECOSM-LSH-CT-503234 (M.Z.).

REFERENCES

1. **Andoh, T., Y. Hirata, and A. Kikuchi.** 2000. Yeast glycogen synthase kinase 3 is involved in protein degradation in cooperation with Bul1, Bul2, and Rsp5. Mol. Cell. Biol. **20:**6712–6720.
2. **Benard, V., and G. M. Bokoch.** 2002. Assay of Cdc42, Rac, and Rho GTPase activation by affinity methods. Methods Enzymol. **345:**349–359.
3. **Bhat, R. V., J. Shanley, M. P. Correll, W. E. Fieles, R. A. Keith, C. W. Scott, and C.-M. Lee.** 2000. Regulation and localization of tyrosine^{216} phosphorylation of glycogen synthase kinase-3β in cellular and animal models of neuronal degeneration. Proc. Natl. Acad. Sci. USA **97:**11074–11079.
4. **Biggs, J., N. Tripoulas, E. Hersperger, C. Dearolf, and A. Shearn.** 1988. Analysis of the lethal interaction between the *prune* and *Killer of prune* mutations of *Drosophila*. Genes Dev. **2:**1333–1343.
5. **Cohen, P., and S. Frame.** 2001. The renaissance of GSK3. Nat. Rev. Mol. Cell Biol. **2:**769–776.
6. **Cordes, N., and D. van Beuningen.** 2003. Cell adhesion to the extracellular matrix protein fibronectin modulates radiation-dependent G2 phase arrest involving integrin-linked kinase (ILK) and glycogen synthase kinase-3β (GSK-3β) *in vitro*. Br. J. Cancer **88:**1470–1479.
7. **Cox, E. A., S. K. Sastry, and A. Huttenlocher.** 2001. Integrin-mediated adhesion regulates cell polarity and membrane protrusion through the Rho family of GTPases. Mol. Biol. Cell **12:**265–277.
8. **D'Angelo, A., L. Garzia, A. André, P. Carotenuto, V. Aglio, O. Guardiola, G. Arrigoni, A. Cossu, G. Palmieri, L. Aravind, and M. Zollo.** 2004. Prune cAMP phosphodiesterase binds nm23-H1 and promotes cancer metastasis. Cancer Cell **5:**137–149.
9. **Doble, B. W., and J. R. Woodgett.** 2003. GSK-3: tricks of the trade for a multi-tasking kinase. J. Cell Sci. **116:**1175–1186.
10. **Eickholt, B. J., F. S. Walsh, and P. Doherty.** 2002. An inactive pool of GSK-3 at the leading edge of growth cones is implicated in Semaphorin 3A signaling. J. Cell Biol. **157:**211–217.
11. **Etienne-Manneville, S., and A. Hall.** 2003. Cdc42 regulates GSK-3β and adenomatous polyposis coli to control cell polarity. Nature **421:**753–756.
12. **Forus, A., A. D'Angelo, J. Henriksen, G. Merla, G. M. Maelandsmo, V. A. Flørenes, S. Olivieri, B. Bjerkehagen, L. A. Meza-Zepeda, F. del Vecchio Blanco, C. Müller, F. Sanvito, J. Kononen, J. M. Nesland, Ø. Fodstad, A. Reymond, O.-P. Kallioniemi, G. Arrigoni, A. Ballabio, O. Myklebost, and M. Zollo.** 2001. Amplification and overexpression of *PRUNE* in human sarcomas and breast carcinomas–a possible mechanism for altering the nm23-H1 activity. Oncogene **20:**6881–6890.
13. **Franca-Koh, J., M. Yeo, E. Fraser, N. Young, and T. C. Dale.** 2002. The regulation of glycogen synthase kinase-3 nuclear export by Frat/GBP. J. Biol. Chem. **277:**43844–43848.
14. **Franco, S. J., M. A. Rodgers, B. J. Perrin, J. Han, D. A. Bennin, D. R. Critchley, and A. Huttenlocher.** 2004. Calpain-mediated proteolysis of talin regulates adhesion dynamics. Nat. Cell Biol. **6:**977–983.
15. **Gabarra-Niecko, V., P. J. Keely, and M. D. Schaller.** 2002. Characterization of an activated mutant of focal adhesion kinase: 'SuperFAK'. Biochem. J. **365:**591–603.
16. **Grimes, C. A., and R. S. Jope.** 2001. The multifaceted roles of glycogen synthase kinase 3β in cellular signaling. Prog. Neurobiol. **65:**391–426.
17. **Haut, M., P. S. Steeg, J. K. Willson, and S. D. Markowitz.** 1991. Induction of nm23 gene expression in human colonic neoplasms and equal expression in colon tumors of high and low metastatic potential. J. Natl. Cancer Inst. **83:**712–716.
18. **Hino, S.-I., T. Michiue, M. Asashima, and A. Kikuchi.** 2003. Casein kinase Iε enhances the binding of Dvl-1 to Frat-1 and is essential for Wnt-3a-induced accumulation of β-catenin. J. Biol. Chem. **278:**14066–14073.
19. **Hirata, Y., T. Andoh, T. Asahara, and A. Kikuchi.** 2003. Yeast glycogen synthase kinase-3 activates Msn2p-dependent transcription of stress responsive genes. Mol. Biol. Cell **14:**302–312.
20. **Huttenlocher, A., M. H. Ginsberg, and A. F. Horwitz.** 1996. Modulation of cell migration by integrin-mediated cytoskeletal linkages and ligand-binding affinity. J. Cell Biol. **134:**1551–1562.
21. **Ikeda, S., S. Kishida, H. Yamamoto, H. Murai, S. Koyama, and A. Kikuchi.** 1998. Axin, a negative regulator of the Wnt signaling pathway, forms a complex with GSK-3β and β-catenin and promotes GSK-3β-dependent phosphorylation of β-catenin. EMBO J. **17:**1371–1384.
22. **Ilic, D., Y. Furuta, S. Kanazawa, N. Takeda, K. Sobue, N. Nakatsuji, S. Nomura, J. Fujimoto, M. Okada, T. Yamamoto, and S. Aizawa.** 1995. Reduced cell motility and enhanced focal adhesion contact formation in cells from FAK-deficient mice. Nature **377:**539–544.
23. **Ivaska, J., L. Nissinen, N. Immonen, J. E. Eriksson, V.-M. Kähäri, and J. Heino.** 2002. Integrin α2β1 promotes activation of protein phosphatase 2A and dephosphorylation of Akt and glycogen synthase kinase 3β. Mol. Cell. Biol. **22:**1352–1359.
24. **Jope, R. S., and G. V. W. Johnson.** 2004. The glamour and gloom of glycogen synthase kinase-3. Trends Biochem. Sci. **29:**95–102.
25. **Kikuchi, A.** 1999. Roles of Axin in the Wnt signalling pathway. Cell. Signal. **11:**777–788.
26. **Kim, D., S. Kim, H. Koh, S.-O. Yoon, A.-S. Chung, K. S. Cho, and J. Chung.** 2001. Akt/PKB promotes cancer cell invasion via increased motility and metalloproteinase production. FASEB J. **15:**1953–1962.
27. **Kishida, S., H. Yamamoto, S.-I. Hino, S. Ikeda, M. Kishida, and A. Kikuchi.** 1999. DIX domains of Dvl and Axin are necessary for protein interactions and their ability to regulate β-catenin stability. Mol. Cell. Biol. **19:**4414–4422.
28. **Klein, P. S., and D. A. Melton.** 1996. A molecular mechanism for the effect of lithium on development. Proc. Natl. Acad. Sci. USA **93:**8455–8459.
29. **Koivisto, L., K. Alavian, L. Häkkinen, S. Pelech, C. A. McCulloch, and H. Larjava.** 2003. Glycogen synthase kinase-3 regulates formation of long lamellipodia in human keratinocytes. J. Cell Sci. **116:**3749–3760.
30. **Kuniyasu, H., W. Yasui, H. Shinohara, S. Yano, L. M. Ellis, M. R. Wilson, C. D. Bucana, T. Rikita, E. Tahara, and I. J. Fidler.** 2000. Induction of angiogenesis by hyperplastic colonic mucosa adjacent to colon cancer. Am. J. Pathol. **157:**1523–1535.
31. **Lesort, M., R. S. Jope, and G. V. W. Johnson.** 1999. Insulin transiently increases tau phosphorylation: involvement of glycogen synthase kinase-3β and Fyn tyrosine kinase. J. Neurochem. **72:**576–584.
32. **Oshiro, T., S. Koyama, S. Sugiyama, A. Kondo, Y. Onodera, T. Asahara, H. Sabe, and A. Kikuchi.** 2002. Interaction of POB1, a downstream molecule of small G protein Ral, with PAG2, a paxillin-binding protein, is involved in cell migration. J. Biol. Chem. **277:**38618–38626.
33. **Ouatas, T., M. Salerno, D. Palmieri, and P. S. Steeg.** 2003. Basic and translational advances in cancer metastasis: Nm23. J. Bioenerg. Biomembr. **35:**73–79.
34. **Parsons, J. T.** 2003. Focal adhesion kinase: the first ten years. J. Cell Sci. **116:**1409–1416.
35. **Plyte, S. E., K. Hughes, E. Nikolakaki, B. J. Pulverer, and J. R. Woodgett.** 1992. Glycogen synthase kinase-3: functions in oncogenesis and development. Biochim. Biophys. Acta **1114:**147–162.
36. **Ridley, A. J., M. A. Schwartz, K. Burridge, R. A. Firtel, M. H. Ginsberg, G. Borisy, J. T. Parsons, and A. R. Horwitz.** 2003. Cell migration: integrating signals from front to back. Science **302:**1704–1709.
37. **Roberts, M. S., A. J. Woods, T. C. Dale, P. van der Sluijs, and J. C. Norman.** 2004. Protein kinase B/Akt acts via glycogen synthase kinase 3 to regulate recycling of αvβ3 and α5β1 integrins. Mol. Cell. Biol. **24:**1505–1515.
38. **Schaller, M. D., J. D. Hildebrand, J. D. Shannon, J. W. Fox, R. R. Vines, and J. T. Parsons.** 1994. Autophosphorylation of the focal adhesion kinase, pp125^{FAK}, directs SH2-dependent binding of pp60^{src}. Mol. Cell. Biol. **14:**1680–1688.
39. **Small, J. V., and I. Kaverina.** 2003. Microtubules meet substrate adhesions to arrange cell polarity. Curr. Opin. Cell Biol. **15:**40–47.
40. **Sobin, L. H., and C. H. Wittekind.** 2002. TNM classification of malignant tumors, 6th ed. Wiley-Liss, Inc., New York, N.Y.
41. **Somanath, P. R., S. L. Jack, and S. Vijayaraghavan.** 2004. Changes in sperm glycogen synthase kinase-3 serine phosphorylation and activity accompany motility initiation and stimulation. J. Androl. **25:**605–617.
42. **Stambolic, V., L. Ruel, and J. R. Woodgett.** 1996. Lithium inhibits glycogen synthase kinase-3 activity and mimics Wingless signalling in intact cells. Curr. Biol. **6:**1664–1668.
43. **Tanji, C., H. Yamamoto, N. Yorioka, N. Kohno, K. Kikuchi, and A. Kikuchi.** 2002. A-kinase anchoring protein AKAP220 binds to glycogen synthase kinase-3β (GSK-3β) and mediates protein kinase A-dependent inhibition of GSK-3β. J. Biol. Chem. **277:**36955–36961.
44. **Thompson, W. J., G. Brooker, and M. M. Appleman.** 1974. Assay of cyclic nucleotide phosphodiesterases with radioactive substrates. Methods Enzymol. **38:**205–212.
45. **Watcharasit, P., G. N. Bijur, J. W. Zmijewski, L. Song, A. Zmijewska, X. Chen, G. V. Johnson, and R. S. Jope.** 2002. Direct, activating interaction between glycogen synthase kinase-3β and p53 after DNA damage. Proc. Natl. Acad. Sci. USA **99:**7951–7955.
46. **Webb, D. J., K. Donais, L. A. Whitmore, S. M. Thomas, C. E. Turner, J. T.**

Parsons, and A. F. Horwitz. 2004. FAK-Src signalling through paxillin, ERK and MLCK regulates adhesion disassembly. Nat. Cell Biol. **6:**154–161.
47. **Webb, D. J., J. T. Parsons, and A. F. Horwitz.** 2002. Adhesion assembly, disassembly and turnover in migrating cells–over and over and over again. Nat. Cell Biol. **4:**E97–E100.
48. **Wodarz, A., and R. Nusse.** 1998. Mechanisms of Wnt signaling in development. Annu. Rev. Cell Dev. Biol. **14:**59–88.
49. **Woodgett, J. R.** 1990. Molecular cloning and expression of glycogen synthase kinase-3/factor A. EMBO J. **9:**2431–2438.
50. **Wozniak, M. A., K. Modzelewska, L. Kwong, and P. J. Keely.** 2004. Focal adhesion regulation of cell behavior. Biochim. Biophys. Acta **1692:**103–119.
51. **Yamamoto, H., M. Ihara, Y. Matsuura, and A. Kikuchi.** 2003. Sumoylation is involved in β-catenin-dependent activation of Tcf-4. EMBO J. **22:**2047–2059.
52. **Yamamoto, H., S. Kishida, T. Uochi, S. Ikeda, S. Koyama, M. Asashima, and A. Kikuchi.** 1998. Axil, a member of the Axin family, interacts with both glycogen synthase kinase 3β and β-catenin and inhibits axis formation of *Xenopus* embryos. Mol. Cell. Biol. **18:**2867–2875.
53. **Yoon, S. O., S. Shin, and A. M. Mercurio.** 2005. Hypoxia stimulates carcinoma invasion by stabilizing microtubules and promoting the Rab11 trafficking of the α6β4 integrin. Cancer Res. **65:**2761–2769.
54. **Yoshimura, T., Y. Kawano, N. Arimura, S. Kawabata, A. Kikuchi, and K. Kaibuchi.** 2005. GSK-3β regulates phosphorylation of CRMP-2 and neuronal polarity. Cell **120:**137–149.
55. **Zollo, M., A. André, A. Cossu, M. C. Sini, A. D'Angelo, N. Marino, M. Budroni, F. Tanda, G. Arrigoni, and G. Palmieri.** 2005. Overexpression of h-prune in breast cancer is correlated with advanced disease status. Clin. Cancer Res. **11:**199–205.